

# The impact of the Jurassic hydrothermal activity on zircon fission track data from the southern Upper Rhine Graben area

Autor(en): **Timar-Geng, Zoltan / Fügenschuh, Bernhard / Schaltegger, Urs**

Objekttyp: **Article**

Zeitschrift: **Schweizerische mineralogische und petrographische Mitteilungen  
= Bulletin suisse de minéralogie et pétrographie**

Band (Jahr): **84 (2004)**

Heft 3

PDF erstellt am: **23.04.2024**

Persistenter Link: <https://doi.org/10.5169/seals-63749>

## **Nutzungsbedingungen**

Die ETH-Bibliothek ist Anbieterin der digitalisierten Zeitschriften. Sie besitzt keine Urheberrechte an den Inhalten der Zeitschriften. Die Rechte liegen in der Regel bei den Herausgebern.

Die auf der Plattform e-periodica veröffentlichten Dokumente stehen für nicht-kommerzielle Zwecke in Lehre und Forschung sowie für die private Nutzung frei zur Verfügung. Einzelne Dateien oder Ausdrucke aus diesem Angebot können zusammen mit diesen Nutzungsbedingungen und den korrekten Herkunftsbezeichnungen weitergegeben werden.

Das Veröffentlichen von Bildern in Print- und Online-Publikationen ist nur mit vorheriger Genehmigung der Rechteinhaber erlaubt. Die systematische Speicherung von Teilen des elektronischen Angebots auf anderen Servern bedarf ebenfalls des schriftlichen Einverständnisses der Rechteinhaber.

## **Haftungsausschluss**

Alle Angaben erfolgen ohne Gewähr für Vollständigkeit oder Richtigkeit. Es wird keine Haftung übernommen für Schäden durch die Verwendung von Informationen aus diesem Online-Angebot oder durch das Fehlen von Informationen. Dies gilt auch für Inhalte Dritter, die über dieses Angebot zugänglich sind.

# The impact of the Jurassic hydrothermal activity on zircon fission track data from the southern Upper Rhine Graben area

Zoltan Timar-Geng<sup>1\*</sup>, Bernhard Fügenschuh<sup>1</sup>, Urs Schaltegger<sup>2</sup> and Andreas Wetzel<sup>1</sup>

## Abstract

The influence of the Jurassic hydrothermal activity on the interpretation of fission track (FT) data from the southern Upper Rhine Graben (URG) is elaborated by means of new zircon FT analyses on samples with known U/Pb crystallisation ages. Zircon FT central ages display a wide spectrum from  $162 \pm 14$  Ma to  $247 \pm 22$  Ma. The combination of the U/Pb ages, independent geologic evidence (such as Mesozoic subsidence history, timing of hydrothermal activity, and apatite FT ages) and the zircon FT data unambiguously indicate a Jurassic thermal overprint in the investigated area. It is suggested that circulating hydrothermal fluids with temperatures in the order of 200–250 °C were responsible for the observed thermal anomaly.

The Jurassic hydrothermal fluid migration appears to have been related to a heating event on a regional scale. Inferences from FT analyses related to burial or denudation history have to take into account how such hydrothermal events affect the FT system, including a changing geothermal gradient with time.

**Keywords:** Black Forest, Vosges, zircon, fission track, partial annealing zone, thermal history.

## Introduction

The Upper Rhine Graben (URG) is the most perceptible part of the European Cenozoic rift system (Fig. 1) that extends from the North Sea into the western Mediterranean. Exhumed Variscan basement is exposed in the Black Forest and the Vosges and forms the flanks of the southern URG.

The emplacement age of volcanic and plutonic rocks in the Vosges was found to be very consistent in the range of 345 to 340 Ma (Schaltegger et al., 1996). In the Central Vosges the granulite-facies metamorphism was dated at about 335 Ma and amphibolite-facies retrograde overprint at about 328 Ma (Schaltegger et al., 1999). The analysed granites and rhyolites in the southern Black Forest yielded emplacement ages of 340 to 332 Ma (Schaltegger, 2000). Late Palaeozoic erosion affected the area, with the notable exception of some intramontane basins (e.g. Diebold, 1989). Thus, the base of the Mesozoic strata rests on Variscan crystalline basement.

While the URG and its Cenozoic evolution have been thoroughly studied in the past decades (e.g. Rothé and Sauer, 1967; Illies and Müller, 1970; Illies and Fuchs, 1974; Fuchs et al., 1987; Pro-

dehl et al., 1995; Schumacher, 2002), much less is known about the Mesozoic geological history of the area. This is partly due to the fact that most of the Mesozoic strata have been eroded. After Variscan folding, uplift and subsequent denudation, the URG area became part of the central European intracontinental basin, which developed since the Permo-Triassic until the end of the Jurassic (Geyer and Gwinner, 1991). Based on interpolated isopach maps (Geyer and Gwinner, 1991) the thickness of the eroded Mesozoic deposits in the URG area is estimated to be at most 1500 m. Towards the end of the Jurassic (e.g. Geyer and Gwinner, 1991) or later (Ziegler, 1990) the URG area was uplifted above sea level.

In the outcrops of crystalline basement many vein-type mineralisations of Mesozoic age are preserved (e.g. von Gehlen, 1987; Wernicke and Lippolt, 1997; see compilation by Wetzel et al., 2003), evidencing a strong hydrothermal activity mainly in Jurassic times.

In the present study we apply zircon fission track (FT) analysis to basement samples from the Vosges and Black Forest, which were already dated by the U/Pb method (Schaltegger et al., 1996, 1999; Schaltegger, 2000) and thus, provide additional information on the thermal history of the

<sup>1</sup> Geologisch-Paläontologisches Institut, Universität Basel, Bernoullistrasse 32, CH-4056 Basel, Switzerland.

\* Present address: Geologisches Institut, Albert-Ludwigs-Universität Freiburg, Albertstr. 23b, D-79104 Freiburg, Germany. <zoltan.timar-geng@geologie.uni-freiburg.de>

<sup>2</sup> Département de Minéralogie, Université de Genève, Rue des Maraîchers 13, CH-1205 Genève, Switzerland.

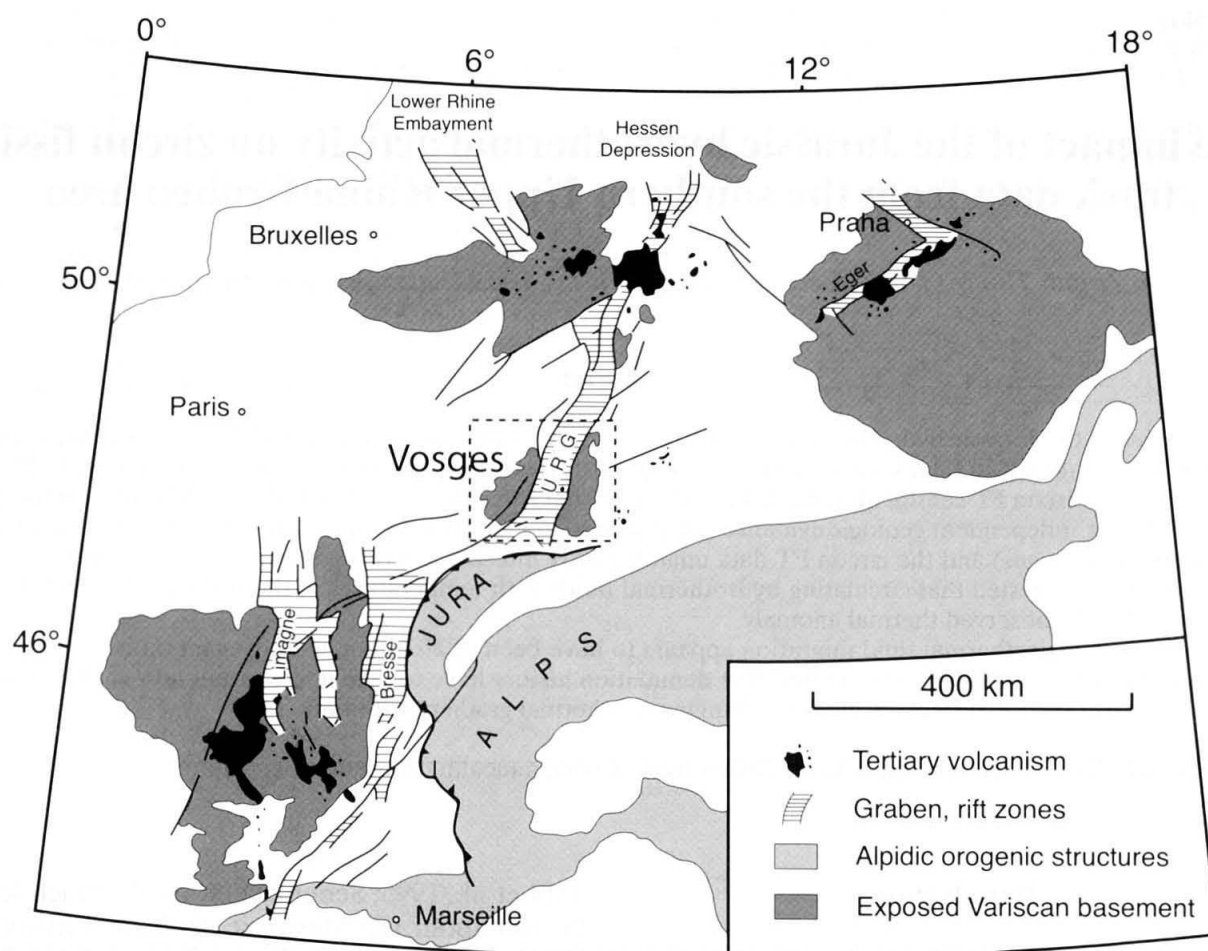


Fig. 1 The Upper Rhine Graben (URG) as part of the European Cenozoic rift system (after Prodehl et al., 1995). Black Forest and Vosges flank the Southern URG. Location of the study area is indicated by dashed square (for details see Figs. 2 and 3).

rocks. Available apatite FT data range from ~37 Ma to ~75 Ma in the Vosges, and ~29 Ma to ~107 Ma in the Black Forest (Michalski, 1987; Hurford and Carter, 1994; Wyss, 2001). Published uplift rates of the Black Forest (Wagner et al., 1989) are inferred from apatite FT data using rather simple assumptions about the paleotemperature field, i.e. constant geothermal gradients. Such an approach may lead to erroneous conclusions about the thermotectonic evolution, if convective heat transport mechanisms changed the temperature field with time. In this study we will focus on the influence of the Jurassic hydrothermal activity on the interpretation of zircon FT data from the Black Forest and Vosges.

### Jurassic hydrothermal activity

In the study area, i.e. the Variscan basement of the Vosges and Black Forest, several prominent hydrothermal events have been reported previously (e.g., Wernicke and Lippolt, 1993; Lippolt and

Kirsch, 1994; see compilation by Wetzel et al., 2003). Two fossil geothermal systems were identified in the intramontane troughs of Baden-Baden, northern Black Forest (Zuther and Brockamp, 1988; Brockamp et al., 1994) and Offenburg, central Black Forest (Brockamp et al., 2003). For these two well documented cases the observed thermal anomaly is clearly related to fault zones and heating effects can be studied in the adjacent rocks (e.g., Brockamp and Zuther, 1983; Brockamp et al., 1987, 1994; Tapfer, 1987; Zuther and Brockamp, 1988; Meyer et al., 2000; Brockamp et al., 2003). In the Baden-Baden trough, Upper Carboniferous, Lower Permian and Triassic sediments were hydrothermally altered during the Jurassic (Zuther and Brockamp, 1988). Vitrinite data indicate that the hydrothermal fluids reached temperatures between 240 and 290 °C (Brockamp and Zuther, 1983). This fossil geothermal system is documented by three distinct alteration zones, including from center to margin, sericitisation, albitisation and weak alteration (Zuther and Brockamp, 1988). K/Ar data on authigenic il-

lites and hydrothermally altered detrital micas reveal two major episodes of fluid migration (Brockamp et al., 1994). The first episode occurred during the Jurassic (150 Ma) and extensively altered the sediments near the fault system of Gernsbach, which is located between the Saxothuringian and Moldanubian zone. The second hydrothermal phase occurred during the Cretaceous (100 Ma) and formed the fluorite-quartz vein-type mineralisation of Käfersteige (Brockamp et al., 1994). In the Offenburg trough, central Black Forest (Brockamp et al., 2003), K/Ar data on sericites point to hydrothermal activity also during the Jurassic (145 Ma). Oxygen isotope data for sericite, sericite composition and vitrinite reflectance investigations indicate hydrothermal fluid temperatures between 150 to 210 °C (Brockamp et al., 2003).

Multiple hydrothermal activities mainly during the Jurassic can be traced around the Pale Atlantic all over western Europe (e.g., Mitchell and Halliday, 1976) suggesting fluid circulation on a wide regional scale. With fluid temperatures in excess of 200 °C at shallow crustal levels, and expecting a pervasive heating of the basement due to continent-wide rifting events during the opening of the North-Atlantic, these hydrothermal events should have substantially altered the paleotemperature field. Thus, interpretation of FT data assuming a constant geothermal gradient leads inevitably to erroneous results.

### Fission track analysis

Zircon FT thermochronology provides insight into the low temperature thermal history of rocks between ~300 °C and ~180 °C, covering the gap between the K/Ar mica and apatite FT dating. Zircon FT analyses were carried out on 21 samples, 14 from the Vosges and 7 from the Black Forest (Figs. 2, 3). For details on lithology and localities the reader is referred to Schaltegger (2000) and Schaltegger et al. (1996, 1999).

### Analytical procedure

Mineral separation and sample preparation followed standard procedures. After mounting in PFA<sup>®</sup> Teflon, zircon grains were polished and etched in a KOH–NaOH eutectic melt at 220 °C for variable times up to 12 h depending on track revelation. Thermal neutron irradiation was carried out at the Australian Nuclear Science and Technology Organisation (ANSTO) facility, Lucas Heights, Australia. All samples were analysed using the external detector method (Naeser, 1976;

Gleadow, 1981). Detector micas were etched for 40 minutes in 40% HF at room temperature. Track counting was performed using an optical microscope ("Axioscope" by Zeiss) with the aid of a computer driven stage (Dumitru, 1993). Magnification was 2500 × using an oil immersion objective. Ages were determined using the zeta approach (Hurford and Green, 1982, 1983) with a zeta value of  $113.49 \pm 1.80$  (Fish Canyon Tuff, CN1). Data processing, error calculation and graphical presentation was performed using free-ware provided by I. Dunkl (2002). All ages are central ages (Galbraith and Laslett, 1993) and errors are quoted at the 1  $\sigma$  confidence level. Results are given in Table 1 according to the I.U.G.S. recommendations (Hurford, 1990).

### Zircon fission track partial annealing zone

In a wide temperature range, known as partial annealing zone (PAZ; Wagner and van den Haute, 1992), fission tracks gradually shorten and eventually disappear completely in response to elevated temperatures over geological timescales.

In case of the apatite FT system the temperature range of the PAZ (~120–60 °C) and the annealing kinetics are well established (e.g. Green et al., 1986; Laslett et al., 1987; Carlson et al., 1999; Donelick et al., 1999; Ketcham et al., 1999). The temperature interval over which FT partial annealing in zircon occurs is, however, still a matter of debate. Early annealing experiments performed on zircon suggest high closure temperatures (exceeding 300 °C) (Fleischer et al., 1965; Krishnaswami et al., 1974; Carpena, 1992) and/or a very broad temperature interval of the PAZ ranging from ~170 to 390 °C (Yamada et al., 1995). Geological constraints on the stability of fission tracks in zircon generally do not confirm such high values. For rocks with a well-established cooling history it is possible to assign a "closure temperature" of the zircon FT system by interpolating the determined FT age. Such calibration yielded effective closure temperatures of ~175 °C (Harrison et al., 1979) and  $240 \pm 50$  °C (Hurford, 1986) for the zircon FT system. Zaun and Wagner (1985) estimated the effective closure temperature to be  $210 \pm 20$  °C on the basis of analysed zircon samples from a borehole section. They interpreted the age reduction with depth as a fossil PAZ. Deep borehole samples from the Vienna Basin revealed no partial annealing in zircons for temperatures up to ~200 °C and a heating duration of the order of 5–10 Ma (Tagami et al., 1996). This information, coupled with a relatively narrow temperature interval of ~230 to ~330 °C for the PAZ (Tagami and Shimada, 1996; Tagami et



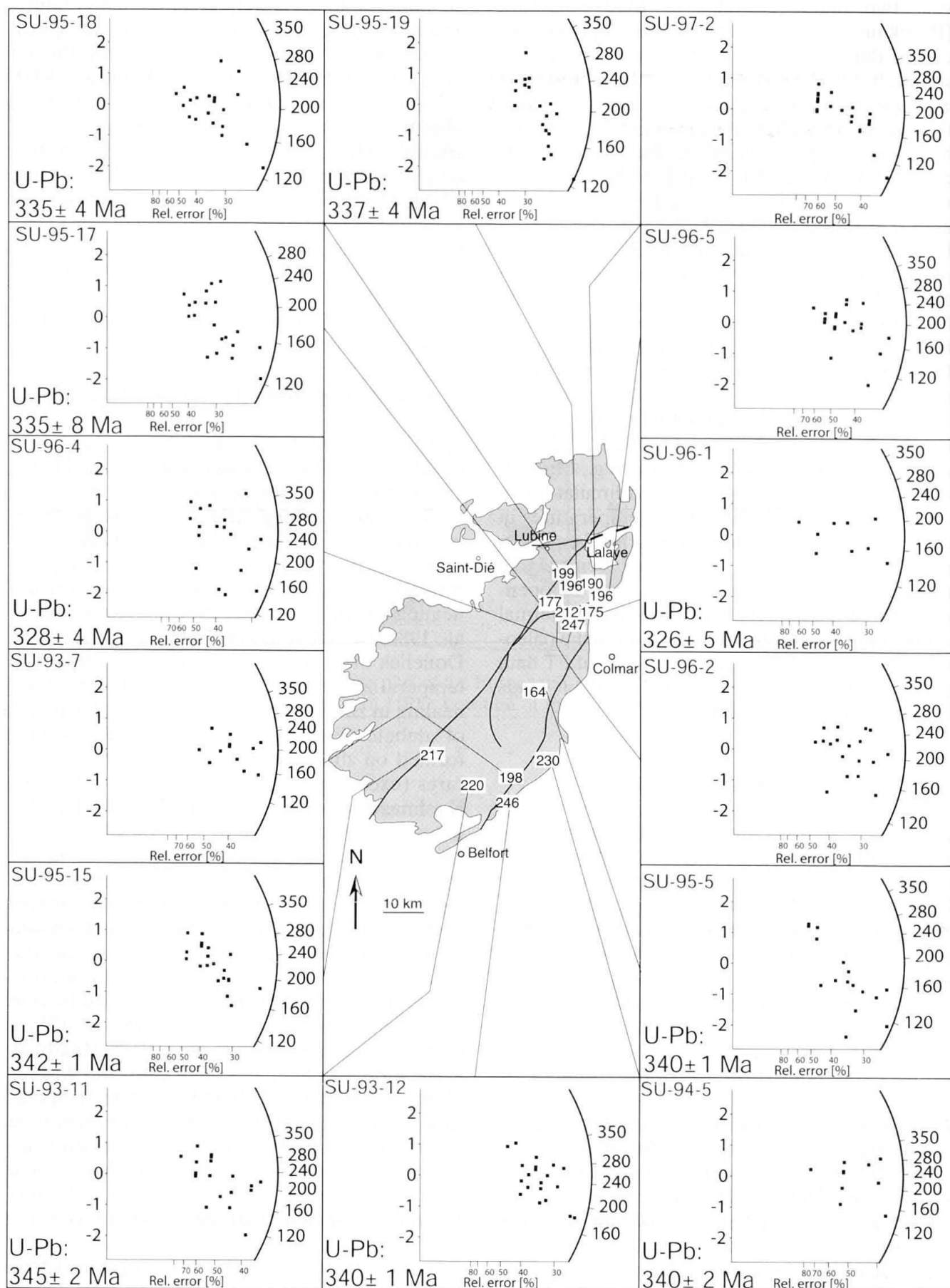


Fig. 2 Zircon FT data from the Vosges. Central ages are plotted on the map. Available U/Pb ages are inserted in the lower left corners of the corresponding radial plots.

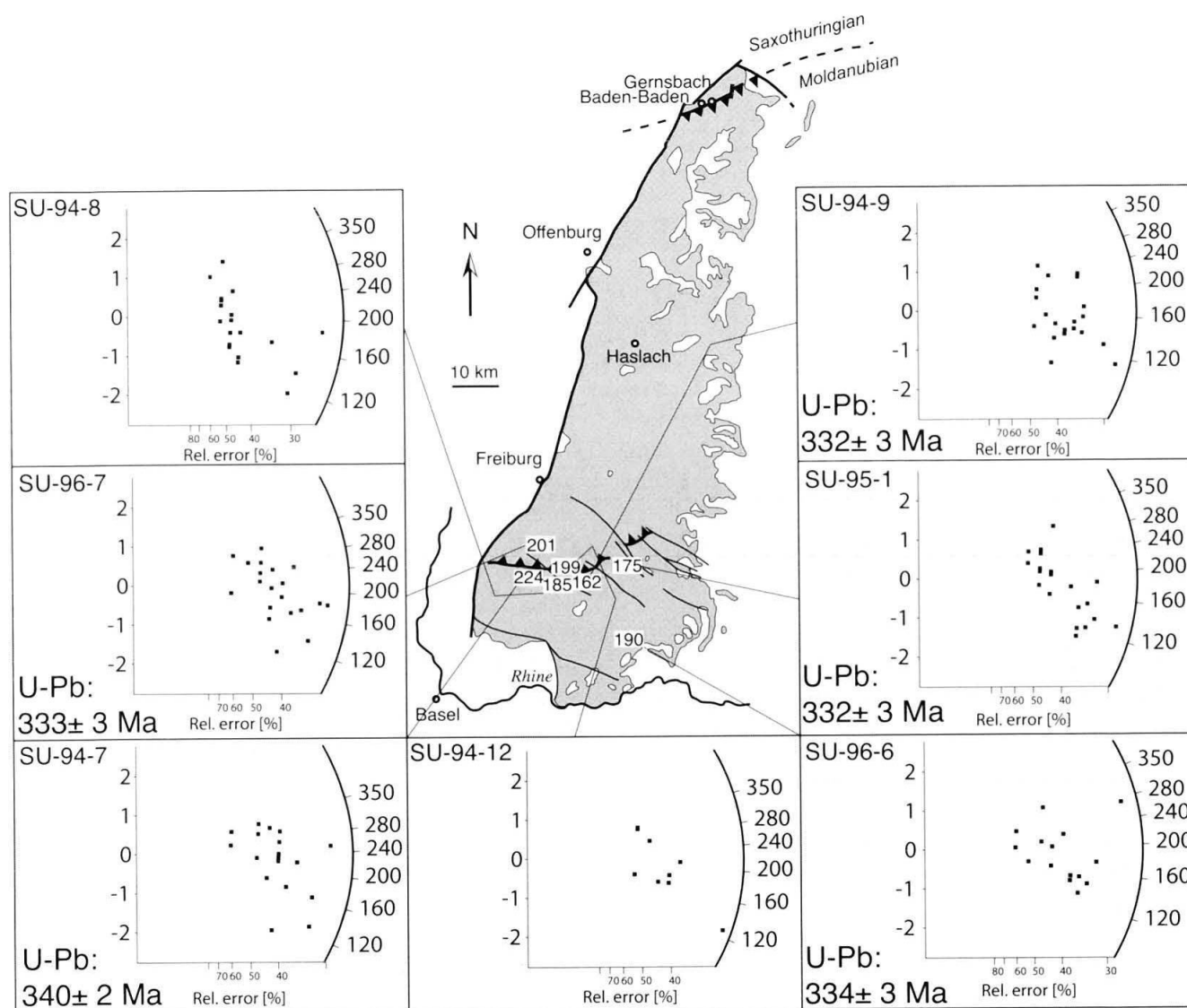


Fig. 3 Zircon FT data (central ages and radial plots) from the Black Forest. Available U/Pb ages are inserted in the lower left corners of the corresponding radial plots.

al., 1998), implies an effective closure temperature of  $280 \pm 50$  °C. The latter value would in principle validate the results of laboratory extrapolations (Yamada et al., 1995) to geological time-scales.

However, experience shows that some kinetic properties of the grains/samples in combination with different thermal histories (fast versus slow cooling) lead to distinct annealing characteristics and hence, give rise to the observed range in (zircon) FT closure temperatures.

In the case of apatite, for example, there is a clear correlation between chemistry and single-grain ages (Green et al., 1986; O'Sullivan and Parrish, 1995) and the higher resistivity of chlorine-rich apatites with respect to fluor-apatites is well known. A similar relationship seemingly exists between the density of accumulated  $\alpha$ -recoil tracks (the damage produced by  $\alpha$ -decay events)

and the single-grain age of zircons (Kasuya and Naeser, 1988; Yamada et al., 1995). This relationship, however, strongly depends on the thermal history of the investigated rocks as the thermal stability of zircon decreases with increasing  $\alpha$  damage (Kasuya and Naeser, 1988). Based on field and laboratory observations Rahn (2001) proposed an  $\alpha$  damage partial annealing zone at higher temperatures than that for the fission tracks in zircons. If a sample cools rapidly through the  $\alpha$  damage PAZ and subsequently through the zircon FT PAZ, no  $\alpha$  damage will be present and thus the annealing of newly forming fission tracks will occur within a pristine lattice. Conversely, samples, which are heated and enter the zircon FT PAZ from the lower temperature side, will have accumulated  $\alpha$  damage over time and the level of this damage will influence the rate of FT annealing (Rahn et al., 2004).

It seems difficult to define a generally applicable zircon FT PAZ because of the manifold dependencies of the annealing characteristics of different samples. As pointed out by Rahn (2001), it is often more appropriate to rely on a "single-grain partial annealing zone" and to define a "sample partial annealing zone" as the integral of partial annealing zones of all grains within a sample. In particular for the determination of the lower temperature boundary of the zircon FT PAZ, it is crucial to independently know the style of the thermal history, i.e. to know whether or not the sample entered the PAZ from the low temperature side. The amount of accumulated radiation damage has important implications for the temperature interval, at which zircon FT annealing occurs.

A compilation of annealing models and geologic constraints (Fig. 4) reveals a broad range for the zircon FT PAZ and reflects its various dependencies on some key parameters such as the cooling rate, the amount of accumulated  $\alpha$  damage and consequently the style of the cooling history.

#### *Single-grain age distributions*

$\chi^2$  statistics (Table 1) indicate that all grains analysed for individual samples belong to a single age population (Green, 1981). Thus, taking a probabil-

ity of less than 5% as evidence for a mixed age population, the observed large spread in single-grain ages does not represent real differences between the apparent ages because  $P(\chi^2)$  values are consistently higher than 5%. The absence of extra-Poissonian variation is also indicated by the radial plots, since all data points scatter within  $\pm 2\sigma$  around the mean. So, from a formal statistical point of view, there is no need to further analyse the single-grain age variation. On the other hand, it has to be noted that the error on all crystals is notably high because of the low number of counted tracks. Thus, the  $\chi^2$  test may have lacked power to detect any extra-Poissonian variation due to the high standard error of the single-grain age estimates and the low number of random samples (generally 20 grains). This can be illustrated assuming we would obtain the same ratio of induced and spontaneous tracks on crystal surfaces ten times greater than the observed ones (Fig. 5). If we calculate the statistics with these new values, the  $\chi^2$  test would fail and we could deal with multiple age populations. Once again, we are fully aware that a statistically founded evaluation of the single-grain age data is not possible. However, after careful consideration of the raw data and relying on our understanding of the underlying processes, we conclude that the observed spread in single-grain ages shows extra-Poissonian variation due to different annealing

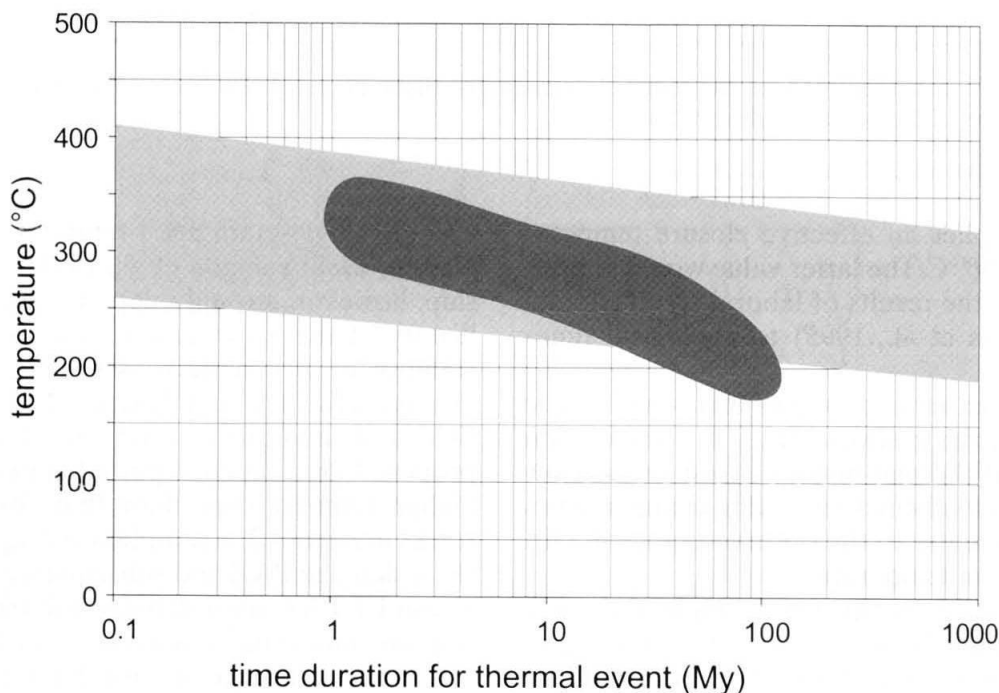


Fig. 4 Constraints on the zircon FT PAZ (modified after Rahn et al., 2004). Light grey: range of the PAZ constrained by fanning annealing models. Dark grey: PAZ derived from geologic evidence. Highest temperatures for the upper (high-temperature) boundary of the PAZ are calculated on the basis of annealing experiments with  $\alpha$  damage-free zircon samples (Rahn et al., 2004). Lowest temperatures are derived from geologic examples with long-duration heating episodes (e.g., Zaun and Wagner, 1985).

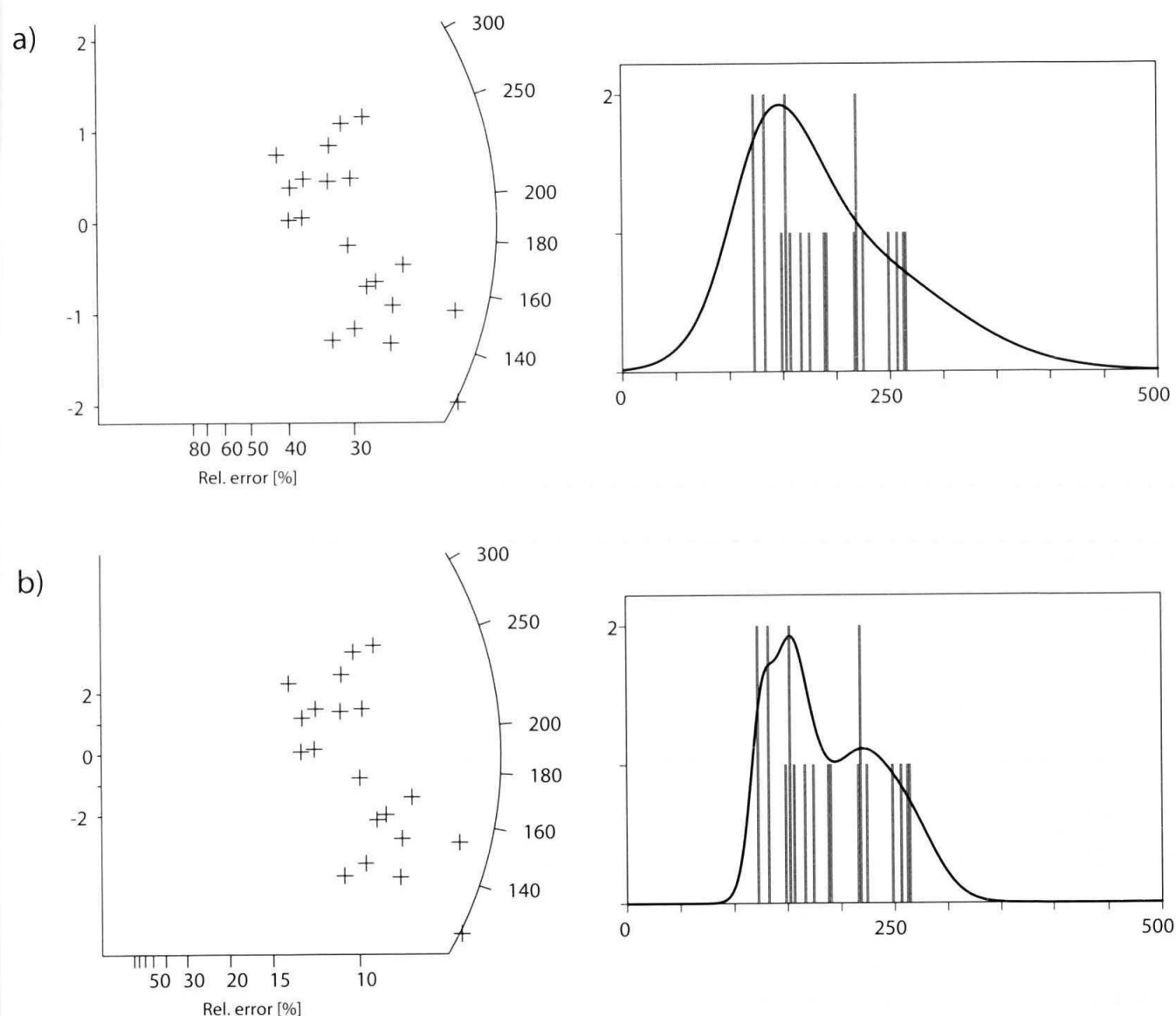


Fig. 5 (a) Radial plot and age-spectrum as probability-density diagram for one sample (SU-95-17) from the Vosges. All single-grain ages plot within  $\pm 2\sigma$  around the mean. (b) Hypothetical plots of the same sample simulating data on ten times greater crystal surfaces ( $N_s \times 10$  and  $N_i \times 10$ , the  $N_s/N_i$  ratio remaining the same). Under this assumption, the single-grain ages show extra-Poissonian variation.

kinetics of the individual grains. This is further evidenced by the fact that none of the samples experienced fast cooling rates and for this reason the individual grains could accumulate different amounts of  $\alpha$  damage causing varying annealing properties of the respective grains (Rahn et al., 2004). Therefore, the following discussion is based on this assumption.

Analyses of single-grain age distributions of detrital zircons have been proven to provide accurate results in exhumation and provenance studies (e.g., Spiegel et al., 2000; Bernet et al., 2001; Stewart and Brandon, 2004). The underlying concept is that recycled sediments may contain zircons derived from various source regions with different thermal histories, thus displaying more than one population of zircon FT ages. However,

a large spread in single-grain age distributions may also occur due to different track retentivity of the individual grains within one sample, for example owing to variable amounts of accumulated  $\alpha$  damage (Kasuya and Naeser, 1988). Over the last decades, several attempts have been made to extract thermochronological information from FT single-grain age data from previously fully or partially annealed samples, based on differential annealing of individual grains (e.g. Green, 1989; Sobel and Dumitru, 1997; Brandon et al., 1998; Fügenschuh and Schmid, 2003). A useful concept is the interpretation of the fraction of zircons with the youngest single-grain ages as those with the lowest thermal stability because they will be the last to close on a cooling path (Brandon et al., 1998). The inference is that the youngest single-



Table 1 Zircon FT data.

| Sample number       | Elevation (m) | No. of crystals counted | Spontaneous tracks $\rho_s$ ( $N_s$ ) | Induced tracks $\rho_i$ ( $N_i$ ) | $P(\chi^2)$ (%) | Dosimeter $\rho_d(N_d)$ | Central age (Ma) $\pm 1\sigma$ |
|---------------------|---------------|-------------------------|---------------------------------------|-----------------------------------|-----------------|-------------------------|--------------------------------|
| <b>Black Forest</b> |               |                         |                                       |                                   |                 |                         |                                |
| SU 94-7             | 920           | 18                      | 201 (1183)                            | 22 (127)                          | 81              | 4.31 (1590)             | 224 $\pm$ 22                   |
| SU 94-8             | 610           | 20                      | 169 (1025)                            | 21 (130)                          | 84              | 4.20 (1590)             | 185 $\pm$ 18                   |
| SU 94-9             | 720           | 20                      | 251 (1256)                            | 33 (163)                          | 94              | 3.75 (1590)             | 162 $\pm$ 14                   |
| SU 94-12            | 560           | 9                       | 287 (462)                             | 37 (59)                           | 73              | 4.54 (1590)             | 199 $\pm$ 28                   |
| SU 95-1             | 980           | 20                      | 222 (1330)                            | 25 (148)                          | 89              | 3.47 (1590)             | 175 $\pm$ 16                   |
| SU 96-6             | 580           | 15                      | 297 (1059)                            | 30 (108)                          | 93              | 3.47 (1605)             | 190 $\pm$ 20                   |
| SU 96-7             | 870           | 20                      | 237 (1315)                            | 24 (133)                          | 96              | 3.64 (1590)             | 201 $\pm$ 19                   |
| <b>Vosges</b>       |               |                         |                                       |                                   |                 |                         |                                |
| SU 93-7             | 690           | 12                      | 395 (936)                             | 38 (90)                           | 100             | 3.40 (1605)             | 198 $\pm$ 23                   |
| SU 93-11            | 700           | 20                      | 177 (993)                             | 18 (99)                           | 97              | 3.92 (1590)             | 219 $\pm$ 24                   |
| SU 93-12            | 460           | 20                      | 418 (1959)                            | 42 (199)                          | 98              | 4.48 (1590)             | 246 $\pm$ 20                   |
| SU 94-5             | 660           | 10                      | 213 (540)                             | 20 (50)                           | 94              | 3.81 (1590)             | 229 $\pm$ 35                   |
| SU 95-5             | 480           | 16                      | 289 (974)                             | 48 (161)                          | 31              | 4.82 (1590)             | 164 $\pm$ 15                   |
| SU 95-15            | 890           | 20                      | 260 (1556)                            | 31 (188)                          | 99              | 4.71 (1590)             | 217 $\pm$ 18                   |
| SU 95-17            | 790           | 20                      | 301 (2241)                            | 35 (260)                          | 71              | 3.66 (1605)             | 177 $\pm$ 13                   |
| SU 95-18            | 400           | 20                      | 246 (1907)                            | 27 (206)                          | 88              | 3.86 (1605)             | 199 $\pm$ 16                   |
| SU 95-19            | 660           | 19                      | 377 (2956)                            | 39 (305)                          | 31              | 3.63 (1590)             | 196 $\pm$ 14                   |
| SU 96-1             | 290           | 9                       | 390 (733)                             | 44 (83)                           | 97              | 3.53 (1605)             | 175 $\pm$ 21                   |
| SU 96-2             | 320           | 18                      | 338 (1914)                            | 33 (188)                          | 96              | 3.72 (1605)             | 212 $\pm$ 17                   |
| SU 96-4             | 480           | 19                      | 278 (1504)                            | 28 (152)                          | 40              | 4.48 (1590)             | 247 $\pm$ 22                   |
| SU 96-5             | 310           | 20                      | 190 (935)                             | 26 (130)                          | 98              | 4.87 (1590)             | 196 $\pm$ 19                   |
| SU 97-2             | 640           | 20                      | 197 (969)                             | 22 (110)                          | 97              | 3.86 (1590)             | 190 $\pm$ 20                   |

Track densities ( $\rho$ ) are in  $10^5$  tracks/cm<sup>2</sup>, number of tracks counted ( $N$ ) shown in brackets.

Analyses by external detector method using 0.5 for the  $4\pi/2\pi$  geometry correction factor.

Ages calculated as central ages according to Galbraith and Laslett (1993) using dosimeter glass CN1 with  $\zeta_{CN1} = 113.49 \pm 1.80$ .

$P(\chi^2)$  is the probability of obtaining  $\chi^2$  value for  $\nu$  degrees of freedom where  $\nu$  = number of crystals – 1.

grain age represents a maximum age for the date when the sample finally left the PAZ (Fig. 6).

## Results

In the Vosges, zircon FT central ages range between  $164 \pm 15$  Ma and  $247 \pm 22$  Ma (Fig. 2, Table 1). No regional trend can be observed.

Very similar results were obtained for the southern Black Forest with zircon FT central ages ranging between  $162 \pm 14$  Ma and  $224 \pm 22$  Ma (Fig. 3, Table 1), with a weak tendency for older ages to be found more to the west of the Black Forest.

Neither for the Black Forest nor for the Vosges a correlation of FT age with altitude could be observed (Fig. 7). An altitude dependence of increasing ages with elevation was not even observed for samples, derived from coherent fault bounded blocks.

Radial plots (Galbraith, 1988, 1990) of analysed samples reveal broad single-grain age variations within individual samples (Figs. 2, 3), however, all samples passed the  $\chi^2$ -test (Green, 1981).

Therefore, from a statistical point of view all samples are characterised by only one grain population. The single-grain ages of each sample, as depicted in the radial plots (Figs. 2, 3), display a broad range from ~340 Ma to ~100 Ma.

All single-grain ages from the Black Forest and Vosges together with the superimposed central ages (Fig. 8) reveal a maximum at ~190 Ma in the Vosges and at ~170 Ma in the Black Forest.

## Discussion

### Pre-Tertiary thermal event in the URG area

The samples from the Black Forest and Vosges have experienced substantial annealing, indicated by the reduced zircon FT central ages with respect to the emplacement ages. Based on independent geological evidence the post-Variscan thermotectonic evolution can be roughly reconstructed. It started with the emplacement of the magmatic rocks at the time, given by the U/Pb ages. Of special interest are samples from volcanic rocks and samples taken close to the base of the

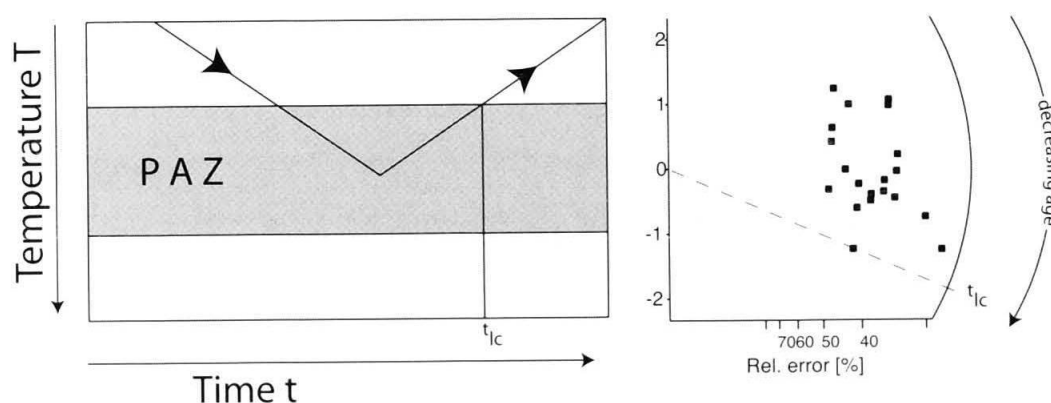


Fig. 6 Thermal history scenario with a thermal peak situated within the PAZ together with a possible single-grain age distribution (after Fügenschuh and Schmid, 2003). The youngest single-grain age corresponds to the time ( $t_{lc}$ ) when the sample cools through the lower limit of the zircon PAZ. For further explanations, see text.

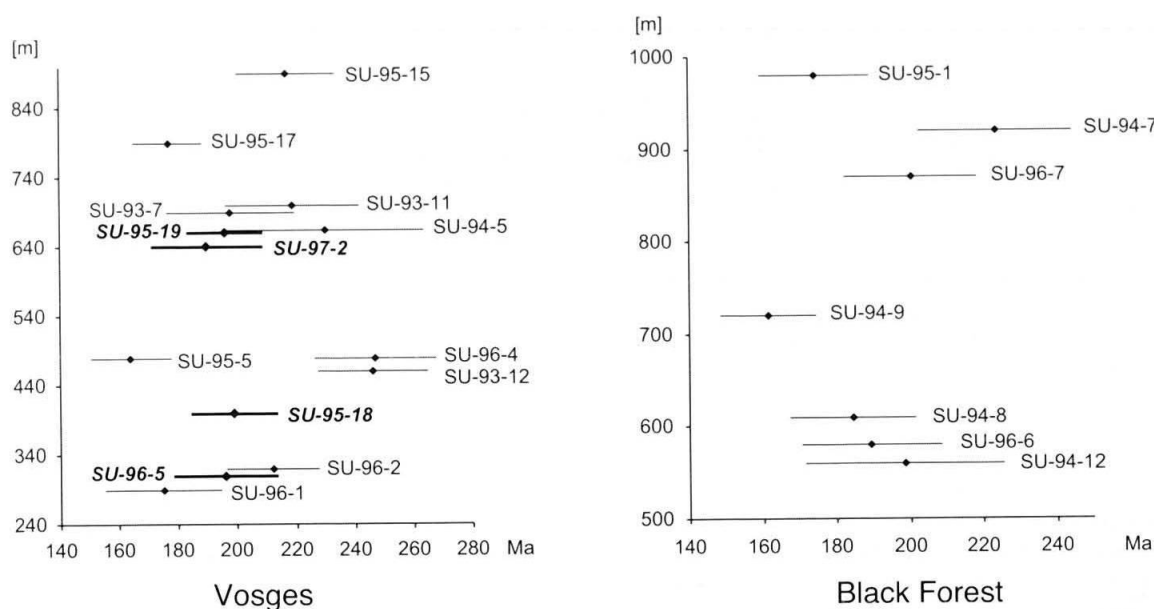


Fig. 7 Age-elevation profiles from the Vosges and the Black Forest. Four highlighted samples from the Vosges (SU 95-18, SU 95-19, SU 96-5 and SU 97-2) indicate that even samples from an apparently homogeneous block do not reveal correlation between the two parameters.

Triassic cover series (e.g. SU-96-6 from the Black Forest). In addition, the Permo-Triassic paleosurface is partly preserved in the Black Forest and has been mapped in the past decades (e.g. Paul, 1955; Wimmenauer and Schreiner, 1990). Thus it is possible to reliably estimate the thickness of the eroded pre-Mesozoic crystalline rocks to be 200 to 600 m, depending on the present elevation of the samples. For the Vosges a similar amount of eroded material is assumed. From the available apatite FT data (Michalski, 1987; Hurford and Carter, 1994; Wyss, 2001), and the youngest zircon FT single-grain ages it is clear that all samples had already cooled to temperatures below the zircon PAZ at  $\sim 100$  Ma. Thus, partial annealing of the zircons must have occurred between the U/Pb ages of 330 Ma and 100 Ma.

Taking the estimated thickness of the Mesozoic sequence into account ( $\sim 1500$  m), the samples have experienced maximum burial of  $\leq 2100$  m (thickness of the Mesozoic sediments +  $\leq 600$  m eroded crystalline basement) at the end of the Mesozoic subsidence phase. Thus, elevated temperatures needed for the observed annealing due to burial alone are impossible to reconcile with the known geology of the region. Interpretation of the zircon FT data using a paleogeothermal gradient of  $30^\circ\text{C}/\text{km}$  would suggest a burial of the present earth's surface of 5–6 km. Instead, the Jurassic hydrothermal fluid migration is suggested to have led to the increased paleotemperatures. The consequence of this convective heat transport seems to have been a heating event of regional extent because its effect can be detected in each of the samples.

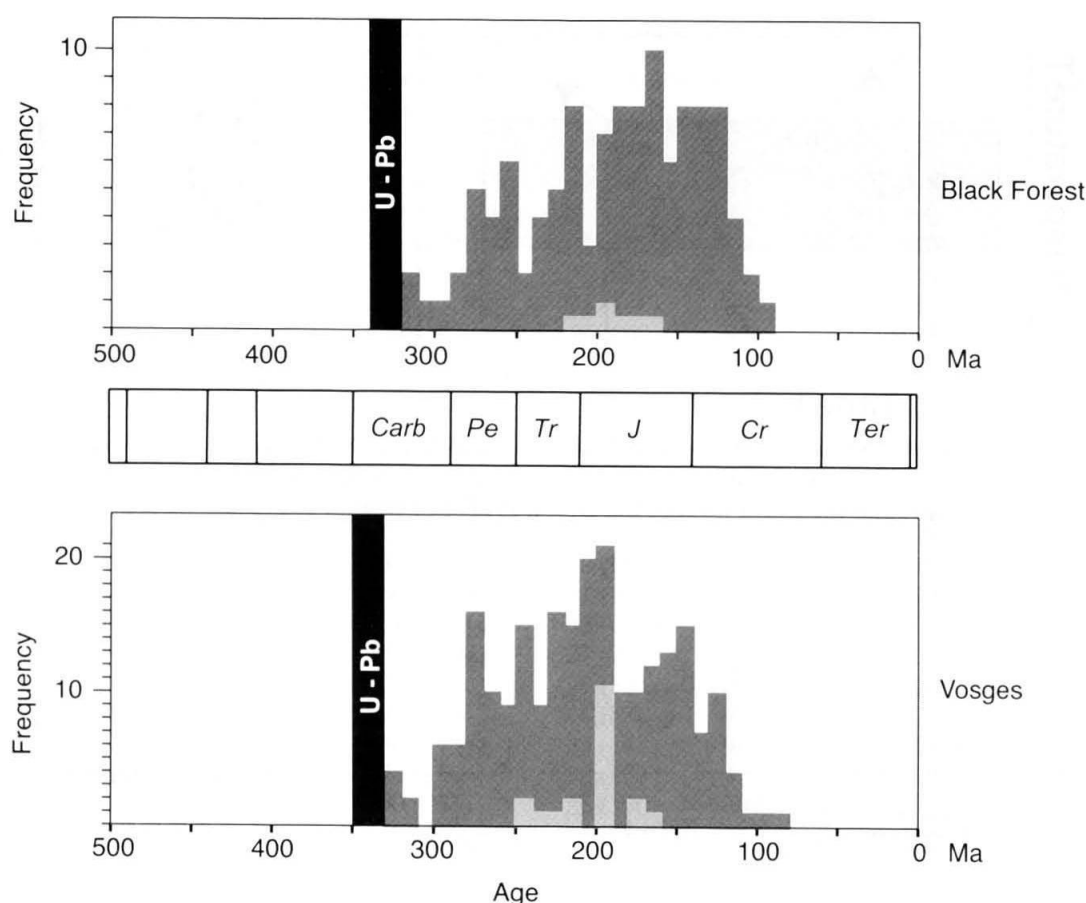


Fig. 8 Frequency distribution of central ages (light grey) and single-grain ages (dark grey) for the whole Vosges and Black Forest regions. Black bars represent the U/Pb ages of the same samples.

Since the samples entered the zircon FT PAZ from the lower temperature boundary after a prolonged period at lower temperatures, a substantial amount of  $\alpha$  damage could be accumulated causing a decreased thermal stability of the zircon fission tracks. Thus, rather moderate temperatures of 200–250 °C would have been sufficient to cause the observed thermal anomaly. Fluid temperatures of this magnitude were reported by Brockamp and Zuther (1983) for the Baden-Baden trough based on vitrinite data. This thermal input is furthermore evidenced by paleomagnetic data from the Southern Vosges (Edel, 1997), documenting post-Permian thermal overprinting.

Zircon FT central ages and single-grain ages from the study area cluster around 190 Ma (Fig. 8). This coincides with the main hydrothermal phase (e.g. Brockamp *et al.*, 1987, 1994; Wernicke and Lippolt, 1993; Lippolt and Kirsch, 1994; see compilation by Wetzel *et al.*, 2003) and one of the most conspicuous subsidence pulses in the investigated area (Wetzel *et al.*, 2003). Furthermore K–Ar data from authigenic illites in sandstones (Schaltegger *et al.*, 1995) and from ore deposits (e.g. Bonhomme *et al.*, 1983) in Europe scatter

around 180–190 Ma. Obviously this was a time period of enhanced fluid flow (illite growth; Schaltegger *et al.*, 1995).

## Conclusions

The analysed samples experienced substantial annealing of fission tracks in zircon prior to Cretaceous cooling. Temperatures needed to allow for the observed annealing cannot be due to burial alone.

Instead, annealing is suggested to be related to a Jurassic thermal pulse, as evidenced by vein mineralisations. A thermal event is independently supported by the well-established hydrothermal activity in the investigated area, although further research is needed to determine the extent of this overprint. However, based on the present study the heating event caused by the Jurassic hydrothermal fluid migration seems to have influenced the upper crust of the southern URG area on a regional scale.

Due to the fact that samples entered the PAZ from the lower temperature boundary and were

only partially annealed, it can be assumed that a high density of  $\alpha$  damage substantially lowered the thermal stability of the zircon fission tracks. Consequently, fluid temperatures in the order of 200–250 °C, as reported for the Jurassic hydrothermal activity in the Baden-Baden and Offenburg troughs (Brockamp and Zuther, 1983; Brockamp et al., 2003), could have been sufficient to substantially alter the palaeotemperature field in the southern URG area.

The impact of the Jurassic hydrothermal activity has important consequences on the interpretation of FT data from the URG area. Analysis of FT data using simple assumptions such as a constant paleogeothermal gradient leads inevitably to erroneous conclusions. The same is also true for the apatite FT system, especially considering that it is even more temperature-sensitive than the zircon FT system. Fluid circulation associated to Cenozoic rifting may have played a substantial role also with respect to apatite FT data. In the light of these results the interpretation of available apatite FT ages from the Black Forest as cooling ages (Michalski, 1987) is also arguable and corresponding uplift rates may have to be revised.

### Acknowledgements

This work has been supported by the Swiss National Science Foundation (Project Nos. 21-57038.99 and 20-64567.01) and is a contribution to the EUCOR-URGENT project. Discussions with B. Schneider and F. Weiss about the statistical treatment of our data greatly improved the manuscript. Critical reviews by I. Dunkl, A. Hurford and an anonymous reviewer are gratefully acknowledged.

### References

- Bernet, M., Zattin, M., Garver, J.I., Brandon, M.T. and Vance, J.A. (2001): Steady-state exhumation of the European Alps. *Geology* **29**, 35–38.
- Bonhomme, M.G., Bühlmann, D. and Besnus, Y. (1983): Reliability of K/Ar-dating of clays and silifications associated with vein mineralizations in western Europe. *Geol. Rundsch.* **72**, 105–117.
- Brandon, M.T., Roden-Tice, M.K. and Garver, J.I. (1998): Late Cenozoic exhumation of the Cascadia accretionary wedge in the Olympic Mountains, northwest Washington State. *Geol. Soc. Am. Bull.* **110**, 985–1009.
- Brockamp, O., Clauer, N. and Zuther, M. (1994): K–Ar dating of episodic Mesozoic fluid migrations along the fault system of Gernsbach within the Moldanubian/Saxothuringian (Northern Black Forest, Germany). *Geol. Rundsch.* **83**, 180–185.
- Brockamp, O., Clauer, N. and Zuther, M. (2003): Authigenic sericite record of a fossil geothermal system: the Offenburg trough, central Black Forest, Germany. *Int. J. Earth Sci.* **92**, 843–851.
- Brockamp, O. and Zuther, M. (1983): Das Uranvorkommen Müllenbach/Baden-Baden, eine epigenetisch-hydrothermale Imprägnationslagerstätte in Sedimenten des Oberkarbon, Teil II: Das Nebengestein. *Neues Jahrb. Mineral. Abh.* **148**, 22–33.
- Brockamp, O., Zuther, M. and Clauer, N. (1987): Epigenetic-hydrothermal origin of the sediment-hosted Müllenbach uranium deposit, Baden-Baden, W-Germany. *Monogr. Ser. Min. Dep.* **27**, 87–98.
- Carlson, W.D., Donelick, R.A., and Ketcham, R.A. (1999): Variability of apatite fission track annealing kinetics I: Experimental results. *Am. Mineral.* **84**, 1213–1223.
- Carpéna, J. (1992): Fission track dating of zircon: zircons from Mont Blanc granite (French-Italian Alps). *J. Geol.* **100**, 411–421.
- Diebold, P. (1989): Der Nordschweizer Permokarbon-Trog und die Steinkohlenfrage der Nordschweiz. *Vjschr. natf. Ges. Zürich* **133/1**, 143–174.
- Donelick, R.A., Ketcham, R.A., and Carlson, W.D. (1999): Variability of apatite fission track annealing kinetics II: Crystallographic orientation effects. *Am. Mineral.* **84**, 1224–1234.
- Dumitru, T.A. (1993): A new computer-automated microscope stage system for fission-track analysis. *Nuclear Tracks and Radiation Measurements* **21**, 575–580.
- Dunkl, I. (2002): Trackkey; a Windows program for calculation and graphical presentation of fission track data. *Computers Geosciences* **28/1**, 3–12.
- Edel, J.-B. (1997): Les reamantations post-permiennes dans le bassin devono-dinantien des Vosges méridionales; existence d'une phase de reamantation au Lias, contemporaine de minéralisations d'ampleur régionale. *Comptes Rendus de l'Académie des Sciences, Paris, Serie II* **324/8**, 617–624.
- Fleischer, R.L., Price, P.B. and Walker, R.M. (1965): Effects of temperature, pressure and ionization on the formation and stability of fission tracks in minerals and glasses. *J. Geophys. Res.* **70**, 1497–1502.
- Fuchs, K., Bonjer, K.-P., Gajewski, D., Lueschen, E., Prodehl, C., Sandmeier, K.-J., Wenzel, F. and Wilhelm, H. (1987): Crustal Evolution of the Rhinegraben area. 1. Exploring the lower crust in the Rhinegraben rift by unified geophysical experiments. *Tectonophysics* **141**, 261–275.
- Fügenschu, B. and Schmid, S.M. (2003): Late stages of deformation and exhumation of an orogen constrained by fission-track data: A case study in the Western Alps. *Geol. Soc. Am. Bull.* **115**, 1425–1440.
- Galbraith, R.F. (1988): Graphical display of estimates having differing standard errors. *Technometrics* **30**, 271–281.
- Galbraith, R.F. (1990): The radial plot: graphical assessment of spread in ages. *Nuclear Tracks and Radiation Measurements* **17**, 207–214.
- Galbraith, R.F. and Laslett, G.M. (1993): Statistical models for mixed fission track ages. *Nuclear Tracks Radiation Measurements* **21**, 459–70.
- Geyer, O.F. and Gwinner, M.P. (1991): Geologie von Baden-Württemberg. 4., neubearb. Aufl. der "Einführung in die Geologie von Baden-Württemberg". Schweizerbart, Stuttgart.
- Gleadow, A.J.W. (1981): Fission track dating methods: what are the real alternatives. *Nuclear Tracks Radiation Measurements* **5**, 3–14.
- Green, P.F. (1981): A new look at statistics in fission track dating. *Nuclear Tracks and Radiation Measurements* **5**, 77–86.
- Green, P.F. (1989): Thermal and tectonic history of the East Midlands shelf (onshore UK) and surrounding regions assessed by apatite fission track analysis. *J. Geol. Soc. London* **146**, 755–773.
- Green, P.F., Duddy, I.R., Gleadow, A.J.W., Tingate, P.R. and Laslett, G.M. (1986): Thermal annealing of fis-



- sion tracks in apatite. 1: A qualitative description. *Chem. Geol.* **59**, 237–253.
- Harrison, T.M., Armstrong, R.L., Naeser, C.W. and Harkal, J.E. (1979): Geochronology and thermal history of the Coast plutonic complex, near Prince Rupert, British Columbia: *Can. J. Earth Sci.* **16**, 400–410.
- Hurford, A.J. (1986): Cooling and uplift patterns in the Lepontine Alps South Central Switzerland and an age of vertical movement on the Insubric fault line. *Contrib. Mineral. Petrol.* **92**, 413–427.
- Hurford, A.J. (1990): International Union of Geological Sciences Subcommittee on Geochronology recommendation for the standardization of fission track dating calibration and data reporting. *Nuclear Tracks and Radiation Measurements* **17/3**, 233–236.
- Hurford, A. and Carter, A. (1994): Regional thermo-tectonic histories of the Rhine Graben and adjacent Hercynian basement: a key to assessing the alpine influence in northwest Europe. 8<sup>th</sup> International Conference on Geochronology, Cosmochronology and Isotope Geology, abstracts, p. 148.
- Hurford, A.J. and Green, P.F. (1982): A users' guide to fission track dating calibration. *Earth Planet. Sci. Lett.* **59/2**, 343–354.
- Hurford, A.J. and Green, P.F. (1983): The zeta age calibration of fission-track dating. *Chem. Geol.* **41/4**, 285–317.
- Illies, J.H. and Fuchs, K. (eds.) (1974): Approaches to Taphrogenesis. Schweizerbart, Stuttgart, 460 pp.
- Illies, J.H. and Müller, St. (eds.) (1970): Graben Problems. Schweizerbart, Stuttgart, 316 pp.
- Kasuya, M. and Naeser, C.W. (1988): The effect of  $\alpha$ -damage on fission-track annealing in zircon. *Nuclear Tracks and Radiation measurements* **14**, 477–480.
- Ketcham, R.A., Donelick, R.A., and Carlson, W.D. (1999): Variability of apatite fission track annealing kinetics III: Extrapolation to geological time scales. *Am. Mineral.* **84**, 1235–1255.
- Krishnaswami, S., Lal, D., Prabhu, N. and MacDougall, D. (1974): Characteristics of fission tracks in zircon: applications to geochronology and cosmology. *Earth Planet. Sci. Lett.* **22**, 51–59.
- Laslett, G.M., Green, P.F., Duddy, I.R. and Gleadow, A.J.W. (1987): Thermal annealing of fission tracks in apatite. 2: A quantitative analysis. *Chem. Geol.* **65**, 1–13.
- Lippolt, H.J. and Kirsch, H. (1994): Isotopic investigation of post-Variscan plagioclase sericitization in the Schwarzwald gneiss massif. *Chemie der Erde* **54**, 179–198.
- Meyer, M., Brockamp, O., Clauer, N., Renk, A. and Zuther, M. (2000): Further evidence for a Jurassic mineralizing event in Central Europe; K–Ar dating of hydrothermal alteration and fluid inclusion systematics in wall rocks of the Kaefersteige fluorite vein deposit in the northern Black Forest, Germany. *Mineralium Deposita* **35/8**, 754–761.
- Michalski, I. (1987): Apatit-Spaltspuren-Datierungen des Grundgebirges von Schwarzwald und Vogesen: Die postvariszische Entwicklung. Unpubl. doctoral dissertation, Heidelberg, pp. 125.
- Mitchell, J.G. and Halliday, A.N. (1976): Extent of Triassic/Jurassic hydrothermal ore deposits on the North Atlantic margin. *Trans. (Sect B) Inst. Min. Metall.* **85**, 159–161.
- Naeser, C.W. (1976): Fission-track dating. *U.S. Geol. Surv., Open-File Rep.* 76-190, 65 pp.
- O'Sullivan, P.B. and Parrish, R.R. (1995): The importance of apatite composition and single-grain ages when interpreting fission track data from plutonic rocks: a case study from the Coast Ranges, British Columbia. *Earth Planet. Sci. Lett.* **132**, 213–224.
- Paul, W. (1955): Zur Morphogenese des Schwarzwaldes (I). *Jahresheft geol. Landesamt Baden-Württ.* **1**, 395–427.
- Prodehl, C., Mueller, S. and Haak, V. (1995): The European Cenozoic rift system. In: K.H. Olsen (ed.): *Continental Rifts: Evolution, Structure, Tectonics. Developments in Geotectonics* **25**, 133–212. Elsevier Sci., New York.
- Rahn, M. (2001): The metamorphic and exhumation history of the Helvetic Alps, Switzerland, as revealed by apatite and zircon fission tracks. Habilitation thesis, University of Freiburg, Germany, 140 pp.
- Rahn, M.K., Brandon, M.T., Batt, G.E. and Garver, J.I. (2004): A zero-damage model for fission-track annealing in zircon. *Am. Mineral.* **89**, 473–484.
- Rothé, J.P. and Sauer, K. (eds.) (1967): The Rhinegraben progress report 1967. *Abh. Geol. Landesamt Baden-Wuerttemberg* **6**, 146 pp.
- Schaltegger, U. (2000): U–Pb geochronology of the Southern Black Forest Batholith (Central Variscan Belt): timing of exhumation and granite emplacement. *Int. J. Earth Sci.* **88**, 814–828.
- Schaltegger, U., Zwingmann, H., Clauer, N., Larque, P. and Stille, P. (1995): K–Ar dating of a Mesozoic hydrothermal activity in Carboniferous to Triassic clay minerals of northern Switzerland. *Schweiz. Mineral. Petrogr. Mitt.* **75**, 163–176.
- Schaltegger, U., Schneider, J.-L., Maurin, J.C. and Corfu, F. (1996): Precise U–Pb chronometry of 345–340 Ma old magmatism related to syn-convergence extension in the Southern Vosges (Central Variscan Belt). *Earth Planet. Sci. Lett.* **144**, 403–419.
- Schaltegger, U., Fanning, C.M., Günther, D., Maurin, J.C., Schulmann, K. and Gebauer, D. (1999): Growth, annealing and recrystallisation of zircon and preservation of monazite in high-grade metamorphism: conventional and in-situ U–Pb isotope, cathodoluminescence and microchemical evidence. *Contrib. Mineral. Petrol.* **134**, 186–201.
- Schumacher, M.E. (2002): Upper Rhine Graben: Role of preexisting structures during rift evolution. *Tectonics* **21/1**, 6/1–17.
- Sobel, E.R. and Dumitru, T.A. (1997): Thrusting and exhumation around margins of the western Tarim Basin during the India-Asia collision. *J. Geoph. Res.* **102**, 5043–5063.
- Spiegel, C., Kuhlemann, J., Dunkl, I., Frisch, W., von Eynatten, H. and Balogh, K. (2000): The erosion history of the Central Alps; evidence from zircon fission track data of the foreland basin sediments. *Terra Nova* **12/4**, 163–170.
- Stewart, R.J. and Brandon, M.T. (2004): Detrital-zircon fission-track ages for the „Hoh Formation“; implications for late Cenozoic evolution of the Cascadia subduction wedge. *Geol. Soc. Am. Bull.* **16**, 60–75.
- Tagami, T. and Shimada, C. (1996): Natural long-term annealing of the zircon fission track system around a granitic pluton. *J. Geophys. Res.* **101/B4**, 8245–8255.
- Tagami, T., Carter, A. and Hurford, A.J. (1996): Natural long-term annealing of the zircon fission-track system in Vienna Basin deep borehole samples: constraints upon the partial annealing zone and closure temperature. *Chem. Geol.* **130**, 147–157.
- Tagami, T., Galbraith, R.F., Yamada, R. and Laslett, G.M. (1998): Revised annealing kinetics of fission tracks in zircon and geological implications. In: Van den Haute, P. and De Corte, F. (eds.): *Advances in Fission Track Geochronology*, Kluwer Academic Publishers, Dordrecht, 99–112.
- Tapfer, M. (1987): Geochemical characteristics of non-strata-bound uranium mineralization of the Muelienbach Deposit (northern Schwarzwald, W. Germany).

- ny). In: Proceedings of the Uranium symposium. *Monograph Series on Mineral Deposits* **27**, 99–106.
- von Gehlen, K. (1987): Formation of Pb–Zn–F–Ba mineralizations in SW Germany: a status report. *Fortschr. Mineral.* **65/1**, 87–113.
- Wagner, G.A., Michalski, I. and Zaun, P. (1989): Apatite fission track dating of the Central European basement. Postvariscan thermo-tectonic evolution. In: Emmermann, R. and Wohlenberg, J. (eds.): *The German Continental Deep Drilling Program (KTB). Site-selection studies in the Oberpfalz and Schwarzwald*. Springer-Verlag, Berlin, 481–500.
- Wagner, G.A. and van den Haute, P. (1992): *Fission-Track Dating*. Kluwer Academic Publishers.
- Wernicke, R.S. and Lippolt, H.J. (1993): Botryoidal hematite from the Schwarzwald (Germany): heterogeneous uranium distributions and their bearing on the helium dating method. *Earth Planet. Sci. Lett.* **114**, 287–300.
- Wernicke, R.S. and Lippolt, H.J. (1997): (U + Th)-He evidence of Jurassic continuous hydrothermal activity in the Schwarzwald basement, Germany. *Chem. Geol.* **138**, 273–285.
- Wetzel, A., Allenbach, R. and Allia, V. (2003): Reactivated basement structures affecting the sedimentary facies in a tectonically „quiescent“ epicontinental basin: an example from NW Switzerland. *Sedimentary Geology* **157**, 153–172.
- Wimmenauer, W. and Schreiner, A. (1990): Erläuterungen zu Blatt 8114, Feldberg. Geol. Karte Baden-Württ. 1:25 000, Stuttgart, 134 pp.
- Wyss, A. (2001): Apatit Spaltspur Untersuchungen in der Vorwaldscholle (SW-Deutschland). Unpubl. diploma thesis, Univ. Basel, 69 pp.
- Yamada, R., Tagami, T., Nishimura, S. and Ito, H. (1995): Annealing kinetics of fission tracks in zircon: an experimental study. *Chem. Geol.* **122**, 249–258.
- Zaun, P.E. and Wagner, G.A. (1985): Fission-track stability in zircons under geological conditions. *Nuclear Tracks and Radiation Measurements* **10**, 303–307.
- Ziegler, P.A. (1990): *Geological Atlas of Western and Central Europe*. Shell Internationale Petroleum Maatschappij – Geological Society Publishing House, 239 pp.
- Zuther, M. and Brockamp, O. (1988): The fossil geothermal system of the Baden-Baden trough (Northern Black Forest, Germany). *Chem. Geol.* **71**, 337–353.

Received 12 November 2003

Accepted in revised form 8 September 2004

Editorial handling: R. Gieré